Variational principle approach to short-pulse laser-plasma interactions in three dimensions

Brian J. Duda and W. B. Mori
Department of Physics and Astronomy, and Department of Electrical Engineering, University of California at Los Angeles, Los Angeles, California 90095

(Received 8 June 1999)

An approach for describing the evolution of short-pulse lasers propagating through underdense plasmas is presented. This approach is based upon the use of a variational principle. The starting point is an action integral of the form $S[a,a^*,\phi]=\int d^4x\ \mathcal{L}[a,a^*,\phi,\partial_\mu a,\partial_\mu a^*,\partial_\mu\phi]$ whose Euler-Lagrange equations recover the well-known weakly nonlinear coupled equations for the envelope of the laser's vector potential a, its complex conjugate a^*, and the plasma wave wakes' (real) potential ϕ. Substituting appropriate trial functions for a, a^*, and ϕ into the action and carrying out the $\int d^2x_\perp$ integration provides a reduced action integral. Approximate equations of motion for the trial-function parameters (e.g., amplitudes, spot sizes, phases, centroid positions, and radii of curvature), valid to the degree of accuracy of the trial functions, can then be generated by treating the parameters as a new set of dependent variables and varying the action with respect to them. Using this approach, fully three-dimensional, nonlinear envelope equations are derived in the absence of dispersive terms. The stability of these equations is analyzed, and the growth rates for hosing and symmetric spot-size self-modulation, in the short-wavelength regime ($k\sim\omega_p/c$) are recovered. In addition, hosing and spot-size self-modulational instabilities for longer wavelength perturbations ($k\ll\omega_p/c$), and an asymmetric spot-size self-modulational instability are found to occur. The relationships between the variational principle formalism, the source-dependent-expansion (SDE), and moment methods are presented. The importance of nonlinear effects is also briefly discussed, and possible directions for future work are given.

PACS number(s): 52.40.Nk, 52.65.−y

I. INTRODUCTION

Studying the evolution of short-pulse high-intensity lasers as they propagate through underdense plasmas is an active area of research due to its importance to some plasma accelerator [1] and radiation schemes [2], as well as for the fast-ignitor fusion concept [3]. Research during the past few years has resulted in the identification of numerous Raman forward scattering (RFS) [4] related instabilities of finite width laser pulses. These include conventional Raman forward scattering [5,6], where the amplitude of the laser becomes unstable, spot-size self-modulation [7–10], where the spot size of the laser becomes unstable, and hosing [11,12], where the centroid of the laser becomes unstable. To study these instabilities separately and to investigate their nonlinear interplay, it is desirable to obtain differential equations for the evolution of the macroscopic quantities that characterize the laser beam profile, such as the amplitude, spot size, phase, radius of curvature, and centroid. There are various methods for attempting to obtain such envelope equations, which include the variational method [13], the moment method [14], and the source-dependent-expansion (SDE) technique [15]. All of these techniques have been successfully used to study relativistic self-focusing [13,15–17], where the laser nonlinearly interacts with the plasma solely through relativistic mass corrections to the quiver motion. However, a laser can also nonlinearly interact with a plasma through its plasma wave wake. In this case, RFS-type instabilities can occur [4]. Of the above methods, only the SDE technique has been used to self-consistently include the effects of the wake on finite width pulses. The SDE technique led to growth rates for spot-size self-modulation [7] and hosing [11] in uniform plasmas.

In this paper we extend the variational principle technique to include the coupling between the laser, the relativistic mass corrections, and the plasma wave. Using the variational principle, we recover the same growth rates for symmetric spot-size self-modulation [7] and hosing [11,12]. However, we have also identified long-wavelength (i.e., perturbations with $k\ll\omega_p/c$) instabilities [18] and an asymmetric spot-size self-modulation instability. In these long-wavelength instabilities, the dominant nonlinear driving term is the relativistic mass correction to the quiver motion rather than the plasma wave wake. Therefore, these instabilities are distinct from the RFS-type instabilities of Refs. [7,11,12], just as relativistic self-phase modulation is distinct from RFS [19]. This distinction is important as it implies that the long-wavelength instabilities can occur at plasma densities between quarter critical and critical densities while the RFS-type cannot.

The variational principle approach presented here more clearly parametrizes the instabilities as nonlinear oscillator couplings between the spot sizes and centroid positions of the laser and the plasma wave wake. This has the advantage that it more clearly demonstrates that the couplings between the laser and wake envelope parameters are the physical mechanisms responsible for the instabilities. In addition, the variational principle seems to be more easily extended to include all of the fluid nonlinearities; it leads naturally to constants of the motion, and it provides for the use of many of the analytic techniques possible with the variational calculus [20]. It is also worth mentioning that the variational approach described here can be extended to other scattering processes such as forward Brillouin scattering.

The outline of this paper is as follows. In Sec. II we describe and outline the variational approach. In addition, to set the stage for the stability analysis, an equilibrium or

zeroth-order solution is obtained. In Sec. III the stability of the zeroth-order solution is analyzed. Previously known instabilities are recovered, and unique physical regimes are predicted. In addition, a totally different three-dimensional asymmetric spot size self-modulation instability is derived. In Sec. IV the relationship between the variational principle approach, the SDE, and the moment method is discussed. Last, in Sec. V, possible directions for future work are given. These include keeping the dispersive terms, using higher order or even the full set of nonlinearities, examining the coupling between the instabilities, using more judicious trial functions, linearizing about more complicated zeroth-order solutions, and including the effects of plasma channels.

II. VARIATIONAL PRINCIPLE METHOD

In the variational approach, a system of partial differential equations is recast in terms of Hamilton's principle—that an action integral, $S=\int d^4x\,\mathcal{L}$, is stationary with respect to independent, first-order variations of the dependent variables. Once the exact Lagrangian density $\mathcal{L}$ for the system is found, an approximate description arises when trial functions with descriptive parameters that depend upon (ψ,τ) are substituted into the action, and the integrations across the transverse coordinates are explicitly performed. This yields a reduced action principle with only (ψ,τ) as the independent variables. In this reduced form of the action integral, the parameters of the trial function represent another set of dependent variables. Varying the action with respect to the new dependent variables yields a set of approximate differential equations for the parameters. The accuracy of this set of equations is determined by the form of the trial function, which can be made arbitrarily accurate by choosing a complete set of special functions with independent amplitudes.

We now motivate the model set of equations for weakly relativistic short pulse laser plasma interactions. We start with the two coupled equations for the density perturbation and normalized vector potential, valid in the weakly relativistic regime, $|a|^2\ll 1$:

$$\left(\frac{\partial^2}{\partial t^2}-c^2\nabla^2\right)\vec{a}=4\pi c\vec{J}_\perp=-\omega_p^2\frac{n}{n_0\gamma}\vec{a}$$
$$=-\omega_p^2\left(1+\delta n-\frac{|a|^2}{2}\right)\vec{a}, \tag{1}$$

$$\left(\frac{\partial^2}{\partial t^2}+\omega_p^2\right)\delta n=c^2\nabla^2\frac{|a|^2}{2}, \tag{2}$$

where $\delta n\equiv(n-n_0)/n_0$. Then, we normalize all time dimensions to ω_p^{-1}, space dimensions to $k_p^{-1}\equiv c/\omega_p$, and make the substitution $a\rightarrow a(x,t)\exp[i(\omega_0 t-k_0 x)]$ with the goal of separating off the fastest time scale. Following this, we make a coordinate transformation to the variables $(\psi\equiv zk_0/\omega_0-t,\tau\equiv z)$. If the transformation was made with $\omega_0\equiv k_0$, we would be mathematically transforming to a set of copropagating coordinates at the speed of light. This is the usual choice in the literature. However, allowing ω_0, and k_0 to be arbitrary as shown, allows for a mathematical description of the envelope in terms of coordinates comoving at the linear group velocity of the pulse v_g where $v_g=k_0/\omega_0$, $\omega_0^2=1+k_0^2$ [16]. Upon switching to the potential $\phi\equiv\delta n-|a|^2/4$, making the envelope approximation $\partial_\tau a\ll k_0 a$, noting that $\vec{a}$ is describable by a single scalar, and dropping derivatives of $|a|^2$ as slow, we arrive at the equations

$$\left[\nabla_\perp^2-2\frac{\partial^2}{\partial\psi\partial\tau}-2ik_0\frac{\partial}{\partial\tau}+\left(1-\frac{k_0^2}{\omega_0^2}\right)\partial_\psi^2-(k_0^2-\omega_0^2)\right]a$$
$$=(1-\phi)a, \tag{3}$$

$$\left(\frac{\partial^2}{\partial\psi^2}+1\right)\phi=\frac{|a|^2}{4}. \tag{4}$$

If the choice $\omega_0\equiv k_0$ is made, so that we are using the traditional light-frame variables, we arrive at the well known set of coupled differential equations for short-pulse laser plasma interactions in the weakly relativistic regime,

$$\left(\nabla_\perp^2-2\frac{\partial^2}{\partial\psi\partial\tau}-2ik_0\frac{\partial}{\partial\tau}\right)a=(1-\phi)a, \tag{5}$$

$$\left(\frac{\partial^2}{\partial\psi^2}+1\right)\phi=\frac{|a|^2}{4}. \tag{6}$$

We next apply the variational principle approach outlined above to these model equations. The action integral for this set of equations is

$$S=\int dx_\perp d\psi d\tau\left[\nabla_\perp a\cdot\nabla_\perp a^*-ik_0(a\partial_\tau a^*-a^*\partial_\tau a)\right.$$
$$+\left(1-\frac{k_0^2}{\omega_0^2}\right)(\partial_\psi a)(\partial_\psi a^*)-(\partial_\psi a\partial_\tau a^*+\partial_\psi a^*\partial_\tau a)$$
$$\left.-2(\partial_\psi\phi)^2+2\phi^2-(\phi-1-k_0^2+\omega_0^2)|a|^2\right]. \tag{7}$$

It can be readily verified that our starting equations are the result of varying the action with respect to a, a^*, and ϕ. From now on, without loss of generality, we choose $\omega_0\equiv k_0$, wherein Eqs. (5) and (6) are the equations of motion. We also drop the mixed partial derivative term, i.e., the so-called dispersive or nonparaxial term, in the equation for a. This term is less important than the others for certain regimes of interest. Neglecting it (when $\omega_0\equiv k_0$) results in conservation of power, which simplifies the analysis greatly. However, these simplifications preclude seeing effects due to traditional one-dimensional (1D) Raman forward scattering [4–6], in which power is not conserved. We will address the consequences of the dispersive term in the context of the variational approach in a forthcoming publication.

We choose the following trial functions for a and ϕ:

$$a=A(\psi,\tau)e^{ik_x(\psi,\tau)\tilde{x}_a}e^{ik_y(\psi,\tau)\tilde{y}_a}$$
$$\times\exp\left(-[1-i\alpha_x(\psi,\tau)]\frac{\tilde{x}_a^2}{w_{xa}(\psi,\tau)^2}\right)$$
$$\times\exp\left(-[1-i\alpha_y(\psi,\tau)]\frac{\tilde{y}_a^2}{w_{ya}(\psi,\tau)^2}\right), \tag{8}$$

$$\phi=\Phi(\psi,\tau)\exp-2\left(-\frac{\tilde{x}_\phi^2}{w_{x\phi}(\psi,\tau)^2}+\frac{\tilde{y}_\phi^2}{w_{y\phi}(\psi,\tau)^2}\right), \quad (9)$$

where $\tilde{x}_a\equiv x-x_a(\psi,\tau)$, $\tilde{y}_a\equiv y-y_a(\psi,\tau)$, $\tilde{x}_\phi\equiv x-x_\phi(\psi,\tau)$, $\tilde{y}_\phi\equiv y-y_\phi(\psi,\tau)$, and the amplitude A is a complex amplitude such that $A(\psi,\tau)=\sqrt{\xi(\psi,\tau)}e^{i\chi(\psi,\tau)}$. Each of the parameters has a well defined interpretation, e.g., w_a represents the spot size, α is related to the radius of curvature, x_a represents the centroid position for a, and x_ϕ represents the centroid position for ϕ, etc. The trial function for a is the same function used in the SDE approach by Sprangle *et al.* [11]. The form of the trial function for ϕ is chosen so as to agree with the fact that in the absence of the ψ derivative term in the equation for the wake, the scalar potential is given by $\phi=|a|^2/4$. It is tempting on this basis to assume that the spot sizes and centroids for ϕ are the same as the spot sizes and centroids for a. However, in order to properly allow for the self-consistent evolution of the plasma wave wake, it is necessary to make the more general assumption, and allow the parameters to be different. If one did assume that the centroids and the spot sizes were the same for the two potentials, one would immediately arrive at a particular regime of the instabilities discussed later in this paper, i.e., the long-wavelength regimes. This point clearly indicates that these regimes are distinct.

We now insert these trial functions into the action integral and perform the $\int d^2x_\perp$ integration—which yields the following reduced action (algebraic details are given in Appendix A):

$$S=\int d\psi\, d\tau\Bigg[P\left(\frac{k_x^2}{2}+\frac{k_y^2}{2}+\frac{(1+\alpha_x^2)}{2w_{xa}^2}+\frac{(1+\alpha_y^2)}{2w_{ya}^2}-k_0(\partial_\tau\chi-k_x\partial_\tau x_a-k_y\partial_\tau y_a)\right)-Pk_0\left[\frac{w_{xa}^2}{4}\partial_\tau\left(\frac{\alpha_x}{w_{xa}^2}\right)+\frac{w_{ya}^2}{4}\partial_\tau\left(\frac{\alpha_y}{w_{ya}^2}\right)\right]+\frac{1}{2}(P$$
$$+w_{x\phi}w_{y\phi}\Phi^2)-\frac{w_{x\phi}w_{y\phi}\Phi P\exp\left[-2\left(\frac{(x_a-x_\phi)^2}{(w_{xa}^2+w_{x\phi}^2)}+\frac{(y_a-y_\phi)^2}{(w_{ya}^2+w_{y\phi}^2)}\right)\right]}{2\sqrt{(w_{xa}^2+w_{x\phi}^2)(w_{ya}^2+w_{y\phi}^2)}}-\left(\frac{w_{x\phi}w_{y\phi}}{2}(\partial_\psi\Phi)^2+\frac{\partial_\psi(\Phi^2)}{4}\partial_\psi(w_{x\phi}w_{y\phi})\right)$$
$$-\frac{\Phi^2}{4}(\partial_\psi w_{x\phi})(\partial_\psi w_{y\phi})-\frac{3}{8}\Phi^2\left(\frac{w_{y\phi}}{w_{x\phi}}(\partial_\psi w_{x\phi})^2+\frac{w_{x\phi}}{w_{y\phi}}(\partial_\psi w_{y\phi})^2\right)-\Phi^2\left(\frac{w_{y\phi}}{w_{x\phi}}(\partial_\psi x_\phi)^2+\frac{w_{x\phi}}{w_{y\phi}}(\partial_\psi y_\phi)^2\right)\Bigg]. \quad (10)$$

We have thus reduced the infinite degrees of freedom from the $\vec{x}_\perp$ variable to 15 degrees of freedom, i.e., P, Φ, χ, α_x, α_y, k_x, k_y, w_{xa}, w_{ya}, $w_{x\phi}$, $w_{y\phi}$, x_a, y_a, x_ϕ, and y_ϕ. Varying the action with respect to χ, α_x, α_y, k_x, and k_y yields the following equations: for $\delta\chi$,

$$\partial_\tau P=0 \quad \text{(power conservation)},$$

for $\delta\alpha_x$,

$$\alpha_x=-\frac{k_0}{4}\partial_\tau(w_{xa}^2),$$

for $\delta\alpha_y$,

$$\alpha_y=-\frac{k_0}{4}\partial_\tau(w_{ya}^2),$$

for δk_x,

$$k_x=-k_0\partial_\tau x_a,$$

and for δk_y,

$$k_y=-k_0\partial_\tau y_a. \quad (11)$$

We can use these equations to eliminate χ, α_x, α_y, k_x, and k_y from the Lagrangian since χ is an ignorable coordinate, and the other equations are generated by variations of the action with respect to the quadratic terms for the particular variable [21]. Dropping the ignorable coordinate χ also requires that P be henceforth treated explicitly as a constant of the motion. Eliminating these variables yields the following simplified form of the Lagrangian:

$$L=P\left[\frac{1}{2}\left(\frac{1}{w_{xa}^2}+\frac{1}{w_{ya}^2}\right)-\frac{k_0^2}{8}[(\partial_\tau w_{xa})^2+(\partial_\tau w_{ya})^2+4(\partial_\tau x_a)^2+4(\partial_\tau y_a)^2]\right]+\frac{w_{x\phi}w_{y\phi}\Phi^2}{2}$$

$$-\frac{w_{x\phi}w_{y\phi}\Phi P\exp\left[-2\left(\frac{(x_a-x_\phi)^2}{(w_{xa}^2+w_{x\phi}^2)}+\frac{(y_a-y_\phi)^2}{(w_{ya}^2+w_{y\phi}^2)}\right)\right]}{2\sqrt{(w_{xa}^2+w_{x\phi}^2)(w_{ya}^2+w_{y\phi}^2)}}-\left[\frac{w_{x\phi}w_{y\phi}}{2}(\partial_\psi\Phi)^2+\frac{\partial_\psi(\Phi^2)}{4}\partial_\psi(w_{x\phi}w_{y\phi})+\frac{\Phi^2}{4}(\partial_\psi w_{x\phi})(\partial_\psi w_{y\phi})\right.$$

$$\left.+\frac{3}{8}\Phi^2\left(\frac{w_{y\phi}}{w_{x\phi}}(\partial_\psi w_{x\phi})^2+\frac{w_{x\phi}}{w_{y\phi}}(\partial_\psi w_{y\phi})^2\right)+\Phi^2\left(\frac{w_{y\phi}}{w_{x\phi}}(\partial_\psi x_\phi)^2+\frac{w_{x\phi}}{w_{y\phi}}(\partial_\psi y_\phi)^2\right)\right]. \tag{12}$$

Variation of this Lagrangian with respect to the remaining parameters yields the desired set of differential equations for their evolution. These equations can then be used to study the stability of the beam profile. The full set of equations is given in Appendix B

III. EQUILIBRIUM SOLUTION: SYMMETRIC SELF-FOCUSING

Next, with a perturbative stability analysis in mind, we choose a zeroth-order equilibrium solution to linearize about. The simplest one is a symmetric laser that does not evolve in ψ (i.e., $\partial_\psi=0$). In particular, we set $w_{xa}=w_{ya}\equiv w_a$, $w_{x\phi}=w_{y\phi}\equiv w_\phi$, with all centroids set to 0. Under these conditions, it is straightforward to show that the equations in Appendix B reduce to

$$w_\phi=w_a,\quad \Phi=\frac{P}{4w_a^2}=\frac{A^2}{4},\quad \partial_\tau^2 w_a-\frac{4}{k_0^2w_a^3}\left(1-\frac{P}{32}\right)=0. \tag{13}$$

Alternatively, one could make the substitution that $w_x=w_y$ for both a and ϕ directly into the reduced Lagrangian and vary with respect to w_a, w_ϕ, and Φ. Equations (13) describe symmetric self-focusing, where there is no coupling to the plasma wave wake, and thus no ψ dependence. From them, we obtain the well known critical threshold for self-focusing, $P/P_{\rm crit}=a_0^2w_a^2/32$ [13,15,16]. For $P=P_{\rm crit}$, we have a matched, stationary beam profile, i.e., w_a remains constant if the initial condition $\partial_\tau w_a=0$ is applied.

IV. STABILITY ANALYSIS

In this section we examine the stability of the symmetric self-focusing solution. We do so by linearizing the equations using the self-focusing beam as the zeroth-order solution. However, we restrict our attention to those solutions where the self-focusing occurs on a much slower time scale than the effects due to the plasma wake, and neglect all derivatives of the zeroth-order solution. This approximation becomes exact when $P/P_{\rm crit}=1$, where the beam is matched, and will be approximately valid when $P/P_{\rm crit}$ deviates from 1, so long as the focusing occurs on a slower time scale than the growth of the instabilities in τ.

The number of algebraic manipulations needed to perform the linearization can be minimized by carrying out the perturbation expansion in the Lagrangian. This is done by expanding it to second order in the perturbation parameter. This quadratic Lagrangian, when varied with respect to the first-order quantities, yields the linearized equations (the first-order terms merely reproduce the zeroth-order equations of motion, and can be dropped, using Hamilton's principle). This process is also useful in that additional insight into the linearized system can be gained by knowing its Lagrangian. It is convenient to define the variables

$$\overline{w}_a\equiv\frac{w_{xa1}+w_{ya1}}{2},\quad \overline{w}_\phi\equiv\frac{w_{x\phi1}+w_{y\phi1}}{2}, \tag{14}$$

$$\Delta w_a\equiv\frac{w_{xa1}-w_{ya1}}{2},\quad \Delta w_\phi\equiv\frac{w_{x\phi1}-w_{y\phi1}}{2}. \tag{15}$$

The quadratic Lagrangian can then be written (algebraic details given in Appendix C)

$$\mathcal{L}=\mathcal{L}_{\rm hos}+\mathcal{L}_{\rm smod}, \tag{16}$$

where

$$\mathcal{L}_{\rm hos}=-\frac{16\tilde{P}}{w_0^4}\left(\begin{array}{c}k_0^2w_0^4[(\partial_\tau x_{a1})^2+(\partial_\tau y_{a1})^2]+4\tilde{P}[(\partial_\psi x_{\phi1})^2+(\partial_\psi y_{\phi1})^2]\\-4\tilde{P}[(x_{a1}-x_{\phi1})^2+(y_{a1}-y_{\phi1})^2]\end{array}\right) \tag{17}$$

and $\mathcal{L}_{\rm smod}$ can be broken up as

$$\mathcal{L}_{\rm smod}=\mathcal{L}_{\Phi^2}+\mathcal{L}_{\Phi\overline{w}}+\mathcal{L}_{\rm sym}+\mathcal{L}_{\rm antisym}, \tag{18}$$

with

$$\mathcal{L}_{\Phi^2}=-\frac{w_0^2}{2}[(\partial_\psi\Phi_1)^2-\Phi_1^2], \tag{19}$$

$$\mathcal{L}_{\Phi\overline{w}}=-\frac{8\tilde{P}}{w_0}[(\partial_\psi\overline{w}_\phi)\partial_\psi\Phi_1-(\overline{w}_a+\overline{w}_\phi)\Phi_1], \tag{20}$$

$$\mathcal{L}_{\rm sym}=-\frac{32\tilde{P}}{w_0^4}\{x_R^2(\partial_\tau\overline{w}_a)^2-(3-\tilde{P})\overline{w}_a^2 +2\tilde{P}[(\partial_\psi\overline{w}_\phi)^2-\overline{w}_\phi^2]\}, \tag{21}$$

$$\mathcal{L}_{\rm antisym}=-\frac{32\tilde{P}}{w_0^4}\{x_R^2(\partial_\tau\Delta w_a)^2-3\Delta w_a^2+\tilde{P}[(\partial_\psi\Delta w_\phi)^2 -\Delta w_\phi^2+2\Delta w_\phi\Delta w_a]\}, \tag{22}$$

where

$$x_R\equiv k_0w_0^2/2,\quad \tilde{P}\equiv P/P_{\rm crit}. \tag{23}$$

Notice that the linearized system naturally breaks up into three decoupled subsystems: one for the centroids, one for the averaged spot sizes and Φ, and one for the antisymmetric differentials between the spot sizes in the x and y directions. These subsystems represent the three normal modes of the system: hosing, symmetric spot-size self-modulation, and antisymmetric spot-size self-modulation. We now look at the properties of these normal modes, and examine their stability.

We start by deriving the linearized equations for each system. Varying the quadratic Lagrangian with respect to the centroids yields the following linearized hosing equations: for δx_{a1},

$$\partial_\tau^2x_{a1}+\frac{P}{P_{\rm crit}}\frac{1}{x_R^2}x_{a1}=\frac{P}{P_{\rm crit}}\frac{1}{x_R^2}x_{\phi1}, \tag{24}$$

and for $\delta x_{\phi1}$,

$$\partial_\psi^2x_{\phi1}+x_{\phi1}=x_{a1}. \tag{25}$$

The equations clearly show that hosing is driven by a coupling between the centroids of the laser and the plasma potential. There is also an identical pair of equations for y_{a_1} and y_{ϕ_1}. Varying $\mathcal{L}_{\rm smod}$ with respect to the average spot sizes and Φ_1 yields the following equations: for $\delta\overline{w}_\phi$,

$$[\partial_\psi^2+1]\left(\Phi_1+\frac{16}{w_0^3}\frac{P}{P_{\rm crit}}\overline{w}_\phi\right)=0, \tag{26}$$

for $\delta\Phi_1$,

$$[\partial_\psi^2+1]\left(\Phi_1+\frac{8}{w_0^3}\frac{P}{P_{\rm crit}}\overline{w}_\phi\right)=-\frac{8}{w_0^3}\frac{P}{P_{\rm crit}}\overline{w}_a, \tag{27}$$

and for $\delta\overline{w}_a$,

$$\left[\partial_\tau^2+\frac{1}{x_R^2}\left(3-\frac{P}{P_{\rm crit}}\right)\right]\overline{w}_a=-\frac{w_0^3}{8x_R^2}\Phi_1. \tag{28}$$

The first two equations can be combined to yield

$$(\partial_\psi^2+1)\Phi_1=-\frac{16}{w_0^3}\frac{P}{P_{\rm crit}}\overline{w}_a, \tag{29}$$

$$(\partial_\psi^2+1)\overline{w}_\phi=\overline{w}_a. \tag{30}$$

These two equations, along with the $\delta\overline{w}_a$ equation, are the symmetric envelope self-modulation equations. However, Eqs (28) and (29) are now decoupled from Eq. (30), so symmetric spot-size self-modulation can be completely described by Eqs. (28) and (29). This implies that the instability is driven by a coupling between Φ_1 and w_a. The spot size of ϕ is not directly involved in the feedback loop for this instability, and is simply determined by the evolution of w_a.

Next, we consider variations to the $\mathcal{L}_{\rm asym}$ part of the Lagrangian. Varying the quadratic Lagrangian with respect to the spot-size differentials yields the following antisymmetric spot-size self-modulation equations: for $\delta\Delta w_\phi$,

$$[\partial_\psi^2+1]\Delta w_\phi=\Delta w_a, \tag{31}$$

and for δw_{xa1},

$$\left[\partial_\tau^2+\frac{3}{x_R^2}\right]\Delta w_a=\frac{1}{x_R^2}\frac{P}{P_{\rm crit}}\Delta w_\phi. \tag{32}$$

Before we look at the properties of each subsystem, we note that all of these systems have some common properties. The coupled differential equations for each mode take the following general form:

$$\partial_\tau^2f+\Gamma_1f=\Gamma_2h, \tag{33}$$

$$\partial_\psi^2h+h=\Gamma_3f, \tag{34}$$

where Γ_1 and Γ_2 are functions which are specified by the zeroth-order solution, and f and h represent arbitrary functions of ψ and τ. We examine the stability of these equations by Fourier analyzing them, i.e., substituting behavior of the form $\exp[i(k\tau+\omega\psi)]$. This is rigorously valid if we assume that Γ_1, Γ_2, and Γ_3 are constant which is strictly true for a matched beam. Doing so yields a linear system with secular determinant,

$$k^2\omega^2-\Gamma_1\omega^2-k^2+(\Gamma_1-\Gamma_2\Gamma_3)=0 \tag{35}$$

and an eigenvector relationship $h=g\Gamma_3/(1-\omega^2)$. The constants Γ_1, Γ_2, and Γ_3 have the properties $\Gamma_1\sim O(1/x_R^2)$, and $\Gamma_2\Gamma_3\sim O(1/x_R^2)$, where $x_R=k_0w_0^2/2$ is the Rayleigh length. In our normalized units, $x_R\gg1$.

We first use this dispersion relation to look at the temporal growth rate vs the wave number of the general system. To analyze the growth behavior of the equations, it is necessary to look at the dispersion relation in terms of the frequency and wave number in laboratory (z,t) coordinates, which amounts to transforming $k=\omega'-k'$, $\omega=\omega'$. We then solve

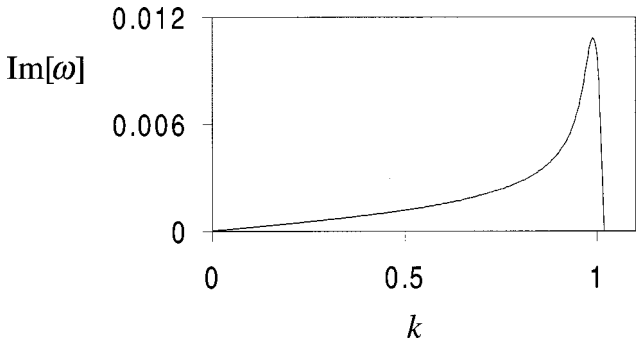

FIG. 1. Hosing temporal growth rate vs wave number for $x_R = 500$, $P/P_{\text{crit}} = 1$.

for the complex ω' as a function of real k'. Figures 1–3 show plots of this solution for each of the three normal modes, using $P/P_{\text{crit}} = 1$, $x_R = 500$ ($k_0 = 10$, $w_0 = 10$), which are easily obtained in experiments [22–26]. For example, this corresponds to a 1-μm laser, $n_0 = 10^{19}\,\text{cm}^{-3}$, $P = 1.7\,\text{TW}$, and $w_0 = 16.8\,\mu\text{m}$.

Certain common properties can be seen from these plots. As previously predicted [11,12] for hosing and symmetric spot-size self-modulation, the growth rates are peaked at $k' = 1$. However, the dispersion relations show that it is possible to see a long-wavelength regime, as demonstrated by the long-wavelength (i.e., small k) tail shown in Figs. 1 and 2. This long-wavelength regime has heretofore never been discussed, and there are reasons to believe that for hosing it is the dominant one in practice, even though it has a lower growth rate [18].

Next, we derive analytic results for this dispersion relation. It is convenient to realize that the Re$[\omega']$ vs k' differs only slightly from a straight line with slope 1, and that the growth rate is also very small. To this end, we write $\omega' = k' + g$, where g is a small complex quantity such that $g \ll k'$, and k' is real. With ω' written this way, the transformation to laboratory coordinates amounts to $k = g$, $\omega = k' + g$. We also note that $x_R \gg 1$, and introduce a small bookkeeping parameter ϵ such that $\epsilon \sim O(1/x_R)$. Finally, defining $\sigma^2 \equiv (P/P_{\text{crit}})/x_R^2$, the secular determinant can be written as

$$g^4 + 2g^3 k' + g^2(k'^2 - 1 - \varepsilon^2\Gamma_1) - 2\varepsilon^2\Gamma_1 g k' - \varepsilon^2\Gamma_1 k'^2 + \varepsilon^2(\Gamma_1 - \Gamma_2\Gamma_3) = 0. \tag{36}$$

We first derive an analytic result for the short-wavelength regime. We expect that the roots we are interested in scale as

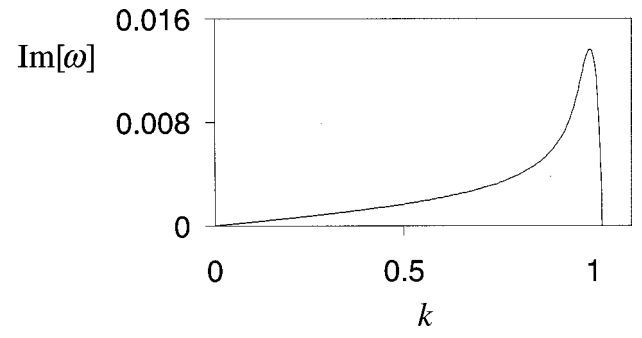

FIG. 2. Symmetric spot-size self-modulation temporal growth rate vs wave number for $x_R = 500$, $P/P_{\text{crit}} = 1$.

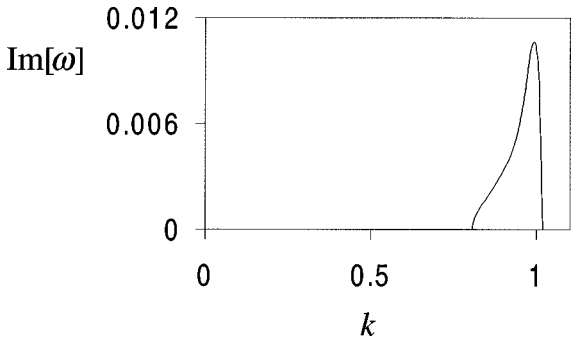

FIG. 3. The antisymmetric spot-size self-modulation temporal growth rate vs wave number for $x_R = 500$, $P/P_{\text{crit}} = 1$.

a positive power of ϵ to lowest order, since $g \ll 1$, as shown in Figs. 1–3. Furthermore, in the short-wavelength regime, k' is near 1, with the peak at 1. To this end, we order the quadratic (in g) coefficient of the dispersion relation as ϵ^2. We then determine the zeroth-order scaling by dominant balance. Pairing off terms, we find that the consistent scaling for the zeroth-order is when cubic and constant terms in the dispersion relation are of the same order, yielding for the peak ($k' = 1$)

$$g = \left(\frac{\Gamma_2\Gamma_3}{2}\right)^{1/3} \frac{(-1 \pm \sqrt{3}i)}{2}. \tag{37}$$

In general, there exists a cutoff, wherein $g = 0$. Setting $g = 0$, we find that the cutoff occurs at

$$k' = \sqrt{\frac{\Gamma_1 - \Gamma_2\Gamma_3}{\Gamma_1}}. \tag{38}$$

When $k' = 0$, we achieve a long-wavelength regime of the sort shown in Figs. 1 and 2. The condition for the long-wavelength regime to occur is thus

$$\Gamma_1 \leqslant \Gamma_2\Gamma_3. \tag{39}$$

In the long-wavelength regime, where $k' \sim O[\epsilon] \ll 1$, we can derive an approximate relation between g and k'. The dominant balance with $k' \sim O[\epsilon]$ is between the largest of the quadratic terms and the constant term, which yields

$$g = i\sqrt{\Gamma_1}k' \tag{40}$$

so that in the long-wavelength regime, the dispersion relation is a straight line with slope $\Gamma_1^{1/2}$. This long-wavelength regime and growth rate could have been obtained immediately by assuming that the centroids and spot sizes of a and ϕ were the same when making the ansatz for the trial functions. With this ansatz, $\partial_\psi^2 \ll 1$, so that $\phi \approx |a|^2/4 - \partial_\psi^2|a|^2/4$. This shows that the long-wavelength regime of the instability is due to relativistic mass corrections, whereas the short-wavelength regime is predominantly a resonant effect caused by density perturbations. While both regimes arise naturally out of this formalism, and continuously merge into each other as a function of k', they are due to distinctly different physical mechanisms. As mentioned earlier, the difference between the long-wavelength and short-wavelength regimes

is analogous to the difference between relativistic self-phase modulation and Raman forward scattering.

It is enlightening to examine the spatial temporal behavior of these instabilities. There are two regimes of interest in this regard: the short-wavelength regime, where $\partial_\psi^2 \sim O(1)$ and the long-wavelength regime, where $\partial_\psi^2 \ll 1$. We now look at the spatial temporal properties of these regimes.

A. The short-wavelength regime

With $\partial_\psi^2 \sim O(1)$, we make the substitutions, $f = \overline{f}\exp[i\psi]$, $g = \overline{h}\exp[i\psi]$, where $\overline{f}$ and $\overline{h}$ are such that $\partial_\psi \overline{f} \ll 1$, $\partial_\psi \overline{h} \ll 1$. Then, neglecting the highest-order derivative in ψ, we obtain

$$\partial_\tau^2 \overline{f} + \Gamma_1 \overline{f} = \Gamma_2 \overline{h}, \tag{41}$$

$$-2i\partial_\psi \overline{h} \simeq \Gamma_3 \overline{f}. \tag{42}$$

Differentiating Eq. (41) with respect to ψ, and substituting Eq. (42), we obtain

$$\partial_\psi \partial_\tau^2 \overline{f} + \Gamma_1 \partial_\psi \overline{f} = \Gamma_2 \Gamma_3 \frac{i\overline{f}}{2}. \tag{43}$$

Here $\partial_\psi \overline{f} \ll \overline{f}$ and $\Gamma_1 \sim O(\Gamma_2 \Gamma_3)$, so we can neglect the $\partial_\psi \overline{f}$ term. Doing so yields

$$(\partial_\psi \partial_\tau^2 - i\gamma)\overline{f} \simeq 0, \tag{44}$$

where $\gamma \equiv \Gamma_2 \Gamma_3/2$. We can now derive the lowest-order asymptotic spatial-temporal growth of this equation, using a stationary phase argument. If we take a complex Laplace transform of this equation using the exponential $\exp[i(k\tau + \omega\psi)]$, the solution can be written in the form

$$\overline{f} = \int d\omega\, dk\, \frac{e^{\Omega(\omega,k)}}{\mathcal{D}(\omega,k)} S(\psi = 0, k), \tag{45}$$

where S is a noise source given by the form of the initial conditions when taking the Laplace transform, $\Omega \equiv i(k\tau + \omega\psi)$, and $\mathcal{D}$ is the dispersion relation for the system, which in this case is given by

$$\mathcal{D} = -i(k^2\omega + \gamma), \tag{46}$$

The exact form of the noise source is not important for our purposes here. The dominant contribution to this integral occurs when $\mathcal{D} \cong 0$ and the argument of the exponent is stationary with respect to ω and k. The value of this stationary exponent gives the lowest order asymptotic spatial-temporal growth rate. Solving the dispersion relation for ω, substituting into the exponential, and requiring that the partial derivative with respect to k be equal to 0 yields

$$k^3 = -\left(\frac{2\gamma\psi}{\tau}\right) \tag{47}$$

or

$$k = -\left(\frac{\Gamma_2\Gamma_3\psi}{\tau}\right)^{1/3}\left\{1, \frac{-1 \pm i\sqrt{3}}{2}\right\}, \tag{48}$$

which yields

$$\Omega = \Gamma_2^{1/3}\psi^{1/3}\tau^{2/3} \times \left\{-i\frac{3}{2}, \pm\frac{\sqrt{3}}{2}\right\} \tag{49}$$

so that the lowest order exponential gain is given by the positive real root

$$\Omega_{res} = \Gamma_2^{1/3}\psi^{1/3}\tau^{2/3}\frac{\sqrt{3}}{2}. \tag{50}$$

B. The long-wavelength regime

In the long-wavelength regime, $\partial_\psi^2 \ll 1$. With this approximation, Eq. (34) can be inverted to yield

$$h = \Gamma_3(1 - \partial_\psi^2) f. \tag{51}$$

Substituting this into Eq. (33) gives

$$[\partial_\tau^2 + \Gamma_2\Gamma_3\partial_\psi^2 + (\Gamma_1 - \Gamma_2\Gamma_3)] f = 0. \tag{52}$$

As noted previously, the long-wavelength regime occurs when $\Gamma_1 \ll \Gamma_2\Gamma_3$. We assume that in addition, $\Gamma_1 - \Gamma_2\Gamma_3 \ll 1$, so that

$$(\partial_\tau^2 + \Gamma_2\Gamma_3\partial_\psi^2) f \cong 0, \tag{53}$$

which yields the dispersion relation

$$k^2 = -\Gamma_2\Gamma_3\omega^2 \tag{54}$$

or

$$k = \pm i\sqrt{\Gamma_2\Gamma_3}\,\omega, \tag{55}$$

so that for a given real ω, we get growth in τ. Therefore, in this long-wavelength regime the perturbations grow as $\exp[(\Gamma_1\Gamma_2)^{1/2}\omega\tau]$. We now use the general results derived herein to examine the properties of each of the three normal modes separately.

C. Hosing

Since hosing is completely decoupled from envelope self-modulation to lowest order, it is instructive to consider the simplest nonlinear extension of the first-order case by holding the spot size fixed, and allowing only the centroids and Φ to evolve in the nonlinear Lagrangian. Making these approximations in the reduced Lagrangian of Eq. (19), and varying with respect to the centroids and Φ yields a nonlinear, coupled set of equations for hosing, which is guaranteed to reduce to the linear equations implied by the quadratic Lagrangian. This approach has the advantage that the nonlinear equations derived by making these variational approximations are easier to digest than the fully nonlinear equations of Appendix A. The nonlinear hosing equations obtained by using Eq. (12) with the aforementioned approximations are as follows: for δx_a,

$$\partial_\tau^2 x_a + \frac{1}{2}\frac{\Phi(x_a - x_\phi)}{k_0^2 w^2}\exp\left(-\frac{(x_a - x_\phi)^2}{w^2}\right) = 0, \tag{56}$$

for δx_ϕ,

$$\Phi^2\partial_\psi^2 x_\phi+\partial_\psi(\Phi^2)\partial_\psi x_\phi-\frac{1}{4}\frac{P\Phi(x_a-x_\phi)}{w^2}\exp\left(-\frac{(x_a-x_\phi)^2}{w^2}\right)=0, \tag{57}$$

for $\delta\Phi$,

$$\partial_\psi^2\Phi+\Phi=2\Phi\left(\frac{(\partial_\psi x_\phi)^2}{w^2}\right)+\frac{P\exp\left[-\left(\frac{(x_a-x_\phi)^2}{w^2}\right)\right]}{2w^2}. \tag{58}$$

Note that we have simplified this analysis further by setting $y_a=y_\phi=0$. Linearizing these equations, or varying the quadratic Lagrangian with respect to the centroids, recovers the linearized hosing equations—Eqs. (24) and (25)— for δx_{a1},

$$\partial_\tau^2 x_{a1}+\frac{P}{P_{\rm crit}}\frac{1}{x_R^2}x_{a1}=\frac{P}{P_{\rm crit}}\frac{1}{x_R^2}x_{\phi 1}, \tag{59}$$

for $\delta x_{\phi 1}$,

$$\partial_\psi^2 x_{\phi 1}+x_{\phi 1}=x_{a1}. \tag{60}$$

Before proceeding, we comment that these two equations can be combined by solving Eq. (60) using a Green's function as

$$x_{\phi 1}(\psi,\tau)=\int_{-\infty}^{\psi}d\psi'\,\sin(\psi-\psi')x_{a1}(\psi',\tau), \tag{61}$$

which upon substituting into Eq. (58) yields

$$\partial_\tau^2 x_{a1}+\frac{P}{P_{\rm crit}}\frac{1}{x_R^2}x_{a1}=\frac{P}{P_{\rm crit}}\frac{1}{x_R^2}\int_{-\infty}^{\psi}d\psi'\times\sin(\psi-\psi')x_{a1}(\psi',\tau). \tag{62}$$

This is identical to Eq. (5) in Ref. [11]. However, when hosing is represented in terms of two coupled equations, Eqs. (24) and (25), rather than a single integral-differential equation, it becomes clearer that hosing results due to a coupling between the centroid positions of a and ϕ. It is also worth noting that equations identical in form to Eq. (62) arise when examining the stability of an electron beam propagating in an ion channel [27]. In this case x_ϕ corresponds to the centroid of the channel and x_a to the centroid of the electron beam. In Ref. [27], the spatial-temporal solutions to such equations are described in detail.

We now look more closely at the properties of the linearized equations. Using the more general analysis in the form of Eqs. (33) and (34), we find that for hosing

$$\Gamma_1=\Gamma_2=\frac{P}{P_{\rm crit}}\frac{1}{x_R^2},\quad \Gamma_3=1. \tag{63}$$

Note that $\Gamma_1=\Gamma_2\Gamma_3$ always, so that a long-wavelength regime exists for all parameters. From Eq. (33) we find that the dispersion relation is

$$k^2\omega^2-\frac{P}{P_{\rm crit}}\frac{1}{x_R^2}\omega^2-k^2=0 \tag{64}$$

with eigenvector relationship $x_{\phi_1}=x_{a_1}/(1-\omega^2)$. Figure 1 shows a plot of this solution for $P/P_{\rm crit}=1$, $x_R=500(k_0=10, w_0=10)$. Note that this dispersion relation shows a clear long-wavelength tail, consistent with the fact that $\Gamma_1=\Gamma_2\Gamma_3$. From Eq. (37) the laboratory frame frequency is

$$g=\left(\frac{1}{2}\frac{P}{P_{\rm crit}}\frac{1}{x_R^2}\right)^{1/3}\frac{(-1\pm\sqrt{3}i)}{2}, \tag{65}$$

The growth rate can then be written

$$\mathrm{Im}[g]=\frac{\sqrt{3}}{4\sqrt[3]{2}}(a_0/k_0 w)^{2/3}.$$

From Eq. (40), the long-wavelength growth rate is

$$g=i\sqrt{\frac{P}{P_{\rm crit}}}\frac{k'}{x_R}. \tag{66}$$

From Eq. (50) the short-wavelength spatial-temporal gain is

$$e^{\Omega_{res}}=\exp\left[\left(\frac{P}{P_{\rm crit}}\frac{1}{x_R^2}\right)^{1/3}\psi^{1/3}\tau^{2/3}\frac{\sqrt{3}}{2}\right]. \tag{67}$$

From Eq. (53), the long-wavelength comoving gain is

$$e^{\Omega_{twh}}=\exp\left[\sqrt{\frac{P}{P_{\rm crit}}}\frac{\omega}{x_R}\tau\right]. \tag{68}$$

It is also worth comparing the linearized equations (24) and (25) to the nonlinear equations (56)–(58). Several features are apparent in the nonlinear version. First, we see that the Gaussian terms that appear in the nonlinear equations will provide a saturation mechanism for the instabilities as the centroid separation gets large. Further, since the Gaussian damping factor evenly multiplies the frequencies in both the δx_a and δx_ϕ equations, we expect that the wave number at which the instability is peaked will downshift to longer wavelengths as the instability saturates. Second, we see that the plasma wave amplitude couples to the nonlinear hosing equations, implying that Raman forward scattering will provide a natural driver for the hosing instability.

D. Symmetric envelope self-modulation

We now use the general results to derive the growth rates for the symmetric spot-size self-modulation instability, which is governed by Eqs. (28) and (29). The Γ parameters for the symmetric instability are

$$\Gamma_1=\frac{1}{x_R^2}\left(3-\frac{P}{P_{\rm crit}}\right),\quad \Gamma_2=-\frac{w_0^3}{8x_R^2},\quad \Gamma_3=-\frac{16}{w_0^3}\frac{P}{P_{\rm crit}}. \tag{69}$$

From Eq. (35) we find that the dispersion relation is

$$\left[k^2\omega^2-\left(3-\frac{P}{P_{\rm crit}}\right)k_R^2\omega^2-k^2+3k_R^2\left(1-\frac{P}{P_{\rm crit}}\right)\right]=0. \tag{70}$$

A plot of this dispersion relation is shown in Fig. 2, for the same parameters used for hosing. Note that we again see a clear long-wavelength tail to the instability, which is similar to what was seen for hosing. This regime has never been

discussed for this instability. It is due to distinctly different physical mechanisms than those that cause the short-wavelength instability, as mentioned previously. This dispersion relation is distinct from the hosing dispersion relation in that it posesses a cutoff which depends on $P/P_{\rm crit}$. This difference arises because $\Gamma_1 \neq \Gamma_2$ and $\Gamma_3 \neq 1$. Although the Fourier analysis is only strictly valid for $P/P_c = 1$, i.e., a matched beam, it is worth examining this cutoff's dependence on P/P_c. From Eq. (38), the cutoff is at

$$k' = \sqrt{3\frac{(1-P/P_{\rm crit})}{3-P/P_{\rm crit}}}. \tag{71}$$

When $P/P_{\rm crit}=1$, we have a complete long-wavelength tail as shown in the plot. This result predicts that when $P/P_{\rm crit} < 1$, there is a cutoff which increases to $k'=1$ as $P/P_{\rm crit} \to 0$. For $1 < P/P_{\rm crit} < 3$, we get an imaginary result, indicating that there is no cutoff at all, and a nonzero growth rate at $k'=0$. This instability is thus related to self-focusing. For $P/P_{\rm crit} > 3$, we again get a real cutoff—which is at $k' \to \infty$ as $P/P_{\rm crit} \to 3+$, and asymptotes to $k' \to \sqrt{3}$ as $P/P_{\rm crit} \to \infty$. This indicates that there is a growth rate which extends beyond $k'=1$ for this region of parameter space, which is physically questionable. The Fourier analysis is valid exactly when $P/P_{\rm crit}=1$, and approximately when $P/P_{\rm crit} \neq 1$, provided that the focusing is still occurring on a much slower time scale than the instability. Since $P/P_{\rm crit} > 3$ in this region of unphysical behavior, these unphysical results should be discarded. Strictly, this dependence of the cutoff on $P/P_{\rm crit}$ should be trusted only near $P/P_{\rm crit}=1$.

The peak temporal (complex frequency) in the short-wavelength regime is [using Eq. (37)]

$$g_{\rm ssm} = \left(\frac{P}{P_{\rm crit}}\frac{1}{x_R^2}\right)^{1/3}\frac{(-1\pm\sqrt{3}i)}{2} = \sqrt[3]{2}\,g_{\rm hos} \tag{72}$$

and is exactly $2^{1/3}$ times the hosing result. The growth rate can then be written

$$\mathrm{Im}[g] = \frac{\sqrt{3}}{4}\left(\frac{a_0}{k_0 w}\right)^{2/3}. \tag{73}$$

From Eq. (40), the long-wavelength laboratory frame frequency is (for $P/P_{\rm crit}=1$)

$$g = i\sqrt{2}\frac{k'}{x_R}. \tag{74}$$

From Eq. (50) the short-wavelength spatial-temporal gain is

$$e^{\Omega_{res}} = \exp\left[\left(2\frac{P}{P_{\rm crit}}\frac{1}{x_R^2}\right)^{1/3}\psi^{1/3}\tau^{2/3}\frac{\sqrt{3}}{2}\right], \tag{75}$$

which is again exactly $2^{1/3}$ times the hosing result. From Eq. (55), the long-wavelength comoving gain is (for $P/P_{\rm crit}=1$ explicitly),

$$e^{\Omega_{\rm wsm}} = \exp\left[\sqrt{2}\frac{\omega}{x_R}\tau\right]. \tag{76}$$

As noted earlier, this is a regime which is the whole beam analog to relativistic self-phase modulation.

We close this section by making connection to the original work of Esarey *et al.* [7]. If we apply the general equations for the short-wavelength regime, Eqs. (41) and (42), to the symmetric spot-size self-modulation instability, and solve Eq. (42) for $\overline{w}_\phi$, we can substitute the solution into Eq. (41). This gives $(\partial_\tau^2 + \Gamma_1)\overline{w}_a = i(\Gamma_2\Gamma_3/2)\int_{-\infty}^{\psi} d\psi' \overline{w}_a$, which is identical to Eq. (4) of Ref. [7], except that here $\Gamma_1 = 3 - P/P_{\rm crit}$, whereas in Ref. [7], $\Gamma_1 = 4 - (5/2)P/P_{\rm crit}$. It appears that the discrepancy is due to an algebraic error in Ref. [7].

E. Antisymmetric envelope self-modulation

We now look at the antisymmetric envelope self-modulation instability in more detail. The linearized equations for this instability are given in Eqs. (31) and (32). These equations show that the instability is driven due to a direct feedback between the spot sizes of a and ϕ, whereas the symmetric spot size instability is driven due to a feedback between Φ_1 and w_a, with w_ϕ uninvolved in the feedback mechanism. This implies that these two instabilities are physically very different. The fact that the magnitude of the longitudinal plasma oscillation couples to the symmetric spot-size modulation implies that this type of modulation can couple directly to Raman forward scattering (if the dispersive cross term was included). In fact, when the dispersive term is included in the analysis, the symmetric instability becomes coupled to modulations to the power, which leads to the formation of a separate branch on the dispersion relation. The asymmetric instability occurs without coupling directly to the magnitude of Φ. It is due to a direct coupling between the side scattering of the plasma wake and the side scattering of the laser field, and is a fundamentally three-dimensional (3D) mode. The lack of a coupling to the magnitude of the plasma wave hints that this process is not coupled to traditional forward Raman scattering. In fact, when the dispersive term is included into our analysis, the laser power is still conserved to first order and there is no additional branch to the dispersion relation. However, the growth rate is modified slightly indicating the presence of additional affects due to the dispersive term. More detail will be given in a forthcoming paper.

We now apply the general stability analysis to this mode to learn more about its properties. The Γ parameters for the antisymmetric instability are

$$\Gamma_1 = \frac{3}{x_R^2}, \quad \Gamma_2 = \frac{1}{x_R^2}\frac{P}{P_{\rm crit}}, \quad \Gamma_3 = 1. \tag{77}$$

From Eq. (35) we find that the dispersion relation is

$$k^2\omega^2 - \frac{3}{x_R^2}\omega^2 - k^2 + \frac{1}{x_R^2}\left(3 - \frac{P}{P_{\rm crit}}\right) = 0. \tag{78}$$

A plot of this dispersion relation is shown in Fig. 3, for the same parameters used for hosing and symmetric spot-size self-modulation. Note that, for these parameters, we see a cutoff, whereas hosing and symmetric spot-size modulation posessed a long-wavelength tail for the same parameters. The cutoff depends upon $P/P_{\rm crit}$, and is given by Eq. (38),

$$k' = \sqrt{1 - \frac{1}{3}\frac{P}{P_{\rm crit}}}. \tag{79}$$

When $P/P_{\rm crit} \to 3$, we obtain a long-wavelength regime. If $P/P_{\rm crit} > 3$, we get an imaginary result, which indicates that there is no cutoff at all, and a nonzero growth rate at $k' = 0$. This implies that an instability due purely to relativistic mass effects, and a type of relativistic self-focusing instability in which the beam focuses asymmetrically, exists at the threshold $P/P_{\rm crit} \to 3$ [17]. In particular, this implies that if the beam self-focuses in the regime $1 < P/P_{\rm crit} < 3$, any small asymmetry will damp away exponentially, whereas if the beam self-focuses when $P/P_{\rm crit} > 3$, the asymmetry will grow exponentially. The peak temporal (complex) frequency in the short-wavelength regime is [using Eq. (37)]

$$g_{\rm assm} = \left(\frac{1}{2}\frac{P}{P_{\rm crit}}\frac{1}{x_R^2}\right)^{1/3}\frac{(-1 \pm \sqrt{3}i)}{2} = g_{\rm hos} \tag{80}$$

and is identical to the hosing result. The growth rate can then be written

$$\mathrm{Im}[g] = \frac{\sqrt{3}}{4\sqrt[3]{2}}\left(\frac{a_0}{k_0 w}\right)^{2/3}. \tag{81}$$

From Eq. (40), the long-wavelength laboratory frame frequency is (for $P/P_{\rm crit} = 3$)

$$g = i\sqrt{3}\frac{k'}{x_R}. \tag{82}$$

From Eq. (50) the short-wavelength spatial-temporal gain is

$$e^{\Omega_{res}} = \exp\left[\left(\frac{P}{P_{\rm crit}}\frac{1}{x_R^2}\right)^{1/3}\psi^{1/3}\tau^{2/3}\frac{\sqrt{3}}{2}\right], \tag{83}$$

which is again identical to the hosing result. From Eq. (55), the long-wavelength comoving gain is (for $P/P_{\rm crit} = 3$ explicitly)

$$e^{\Omega_{\rm wsm}} = \exp\left[\sqrt{3}\frac{\omega}{x_R}\tau\right]. \tag{84}$$

V. VARIATIONAL PRINCIPLES, MOMENT METHODS, AND THE SOURCE-DEPENDENT EXPANSION

In this section we comment on the similarities and differences between the variational, moment, and SDE methods. We begin by examining the variational procedure, with an eye toward a comparison to the other methods. Consider the action integral

$$S[\phi_i(\psi,\tau,x_\perp)] = \int d\psi\, d\tau\, d^2x_\perp \mathcal{L}, \tag{85}$$

which is a functional of a set of fields $\phi_i(\psi,\tau,\mathbf{x}_\perp)$. The equations of motion of the system are generated using Hamilton's principle—that independent variations of the action with respect to the dependent field variables vanishes to first order. Formally, the first variation of the action may be written (using the functional derivative notation of Killingbeck and Cole [19]):

$$\delta S = \int d\psi\, d\tau\, d^2x_\perp \sum_i \left(\frac{\delta S}{\delta \phi_i}\delta\phi_i\right) = 0 \tag{86}$$

which, by the fundamental lemma of the calculus of variations, requires that the first functional derivative of S be equal to 0. This requirement generates the equations of motion of the system, i.e.,

$$\frac{\delta S}{\delta \phi_i} \equiv \frac{\partial \mathcal{L}}{\partial \phi_i} - \partial_j\left(\frac{\partial \mathcal{L}}{\partial(\partial_j \phi_i)}\right) = 0. \tag{87}$$

Now, we insert approximate trial functions into this varied form of the action. Writing

$$\phi_i \approx \tilde{\phi}_i(\beta_k(\psi,\tau),\vec{x}_\perp), \tag{88}$$

where the β_k are the parameters of the trial function, (e.g., ξ, χ, w, α, etc.) and the $\sim$ denotes that the form of ϕ is approximate, we have

$$\delta\phi_i \approx \sum_k \frac{\partial\tilde{\phi}_i}{\partial\beta_k}\delta\beta_k. \tag{89}$$

Then, upon insertion of this representation into the varied form of the action, we find

$$\begin{aligned}\delta S = \int d\psi\, d\tau \sum_j \Bigg[\int d^2x_\perp \sum_i \left(\frac{\delta S}{\delta\phi_i}\bigg|_{\phi_i=\tilde{\phi}_i}\frac{\partial\tilde{\phi}_i}{\partial\beta_j(\psi,\tau)}\right)\Bigg] \\ \times \delta\beta_j(\psi,\tau) \\ = 0,\end{aligned} \tag{90}$$

which means, by the fundamental lemma of the variational calculus, that the equations of motion for the parameters are

$$\int d^2x_\perp \sum_i \left(\frac{\delta S}{\delta\phi_i}\bigg|_{\phi_i=\tilde{\phi}_i}\frac{\partial\tilde{\phi}_i}{\partial\beta_j}\right) = 0, \tag{91}$$

where the trial functions have been inserted into the original equations of motion, denoted by $\delta S/\delta\phi_i$. Note that each term in the sum appearing in Eq. (91) is not necessarily 0 anymore, since the trial function is no longer an exact solution. If a sum over a complete set of functions were chosen as the trial function, we would have an exact representation, and each term in the sum would equal 0. Note that we have one equation for each parameter, and thus have a closed system of equations.

Equation (91) provides a useful calculational tool, and can be applied directly to any system of partial differential equations at the level of the equations of motion, without knowing the particular Lagrangian (provided that one exists) if one knows which equations result from functionally differentiating the action with respect to which dependent variables. In the particular case that no Lagrangian can be found for the specific set of equations, Eq. (91) still suggests a general procedure for generating envelope equations. When an action principle does not exist, it is *usually* due to a few offending terms in certain equations, for which there are no ''Frechet symmetric'' terms [28,29] in the other equations that would allow for the formulation of a varia-

tional principle. Nevertheless, one has in mind what the Lagrangian would be if those extra terms were present, and thereby also knows which equations would be produced due to variations of the action with respect to which dependent variables. In these situations, Eq. (91) implies the following procedure for generating envelope equations: temporarily add in whatever terms are needed to the system of equations so that it is clear which equation is obtained by varying a particular variable, but drop those extra terms just before substituting the trial functions into Eq. (91). A very general exposition on the formulation of variational principles is given in Refs. [29,30].

With the variational method expressed in the form of Eq. (91), we can make a direct comparison between the variational method, the moment method, and the source-dependent expansion. All of these methods require substituting trial functions into linear combinations of the equations of motion, which are then multiplied by linear combinations of the trial functions in some way, and then integrated over the transverse coordinates. This is exactly the form we have here as well. For a Gaussian trial function, it is easy to see that the methods are equivalent. In cylindrical coordinates, each method involves multiplying the equations by a Gaussian times even powers of r^2, and integrating over the transverse coordinates. For the moment method, this is simply a definition of the moment. For the variational method, this comes from differentiating the trial function with respect to α or w, whereas in the SDE, the multiplying factor is simply represented by the Laguerre polynomials.

For the nonlinear Schrodinger equation, the equivalence of the moment method and the variational method for the lowest order Gaussian mode was shown by Anderson and Bonnedal [13]. It can be shown that for the case of the nonlinear Schrodinger equation, the variational method and the source-dependent expansion are exactly equivalent for an arbitrary number of Hermite-Gaussian modes. However, the envelope equations generated by each method are not identical, but are linear combinations of each other.

The complete equivalence is not as clear when the model equations are coupled partial differential equations, rather than a single equation, such as the nonlinear Schrodinger equation. However, the linearized results obtained in this paper for our system of two equations and very specific trial functions agree with results obtained using the source-dependent expansion [7,11]. It is worth noting that Esarey *et al*. did not use a trial function for ϕ, but solved Eq. (6) exactly in terms of $|a|^2/4$.

We close this section by commenting on the work of Shvets and Wurtele [12]. In this work they considered pulses propagating in plasma channels in which the beam is matched, i.e., the spot size does not evolve. They expanded the laser in terms of Laguerre-Gaussian modes. In this case, no centroid position was explicitly included in the Gaussian. Therefore, hosing manifests itself as the growth of the higher-order azimuthally asymmetric Laguerre modes. This approach could be recovered from the variational method if the same modal expansion was used in the trial function. We have also recovered this result using the moment method with Hermite Gaussian modes. We comment that in Ref. [12] the relativistic mass corrections were neglected. As a result, their final dispersion relation does not give any long-wavelength regime which again shows the distinction between the long- and short-wavelength regimes.

VI. SUMMARY

In summary, we have developed a variational approach for studying the evolution of short-pulse laser-plasma interactions. This approach yields coupled envelope equations for macroscopic parameters which describe the laser and the plasma potential. In this paper we have dropped terms arising from dispersion, and concentrated on the linearized version of the resulting equations. The resulting stability analysis predicts three types of whole beam instabilities. In the first, the centroid of the laser couples to the centroid of the plasma potential, i.e., hosing. In the second, the average spot size of the laser is coupled to the amplitude of the plasma potential, i.e., symmetric spot-size self-modulation. In the third, the asymmetry of the laser's spot sizes couples to the asymmetry of the plasma potential's spot sizes, i.e., asymmetric spot-size self-modulation. Each of these instabilities has two basic regimes: a short-wavelength regime and a long-wavelength regime. In the short-wavelength regime, the plasma potential is dominated by the plasma wave wake and oscillates near ω_p. These are the whole beam analogs of RFS [4,5]. The RFS regimes of hosing and symmetric spot-size self-modulation had been previously predicted. The variational calculations also predict a new asymmetric spot-size self-modulation instability. In the long-wavelength regime, the modulations to the plasma potential are dominated by the relativistic mass corrections, i.e., the ponderomotive potential. These regimes are the whole beam analogs to relativistic self-phase modulation (RSPM) and are distinct from the RFS regimes in the same way that RSPM is distinct from RFS.

There are many directions for future work, the most apparent of which is to keep the dispersive terms. Their importance is already well documented. We will address how the dispersive terms modify the growth rates and introduce new instabilities in a future publication. For laser drivers in plasma-based acceleration, it would be useful to include the terms from a plasma channel. Another area of future work is to examine the nonlinear coupling between instabilities, e.g., hosing in the presence of an existing plasma wave. Yet another is to perturb about a different equilibrium profile, e.g., a beam with an elliptical cross section. For example, we have already considered how the results change in slab geometry. In this case the growth rate for hosing is reduced by a factor of $1/\sqrt{2}$. One could also examine the effect of trial functions with higher-order Hermite-Gaussian modes included. Another possibility would be to study the full set of nonlinearities. This is possible in principle by using the Lagrangians published by Chen and Sudan [16] or Brizaird [31]. The main difficulty in this regard is in carrying out the transverse integrations once the form of a Gaussian-based trial function is inserted into the action. Towards this goal, we have already derived a fully nonlinear Lagrangian which is amenable to the use of trial functions. Last, we point out that a similar variational approach could be applied to other types of laser-plasma interactions such as the coupled forward Brillouin scattering and ponderomotive self-focusing instability. We have recently done this successfully [32].

ACKNOWLEDGMENTS

This work was partially supported under the auspices of the U.S. Department of Energy by the Lawrence Livermore National Laboratory, through the Institute for Laser Science and Applications, under Contract No. W-7405-ENG-48. This work was also supported by DOE Grant Nos. DE-FGO3-92ER40727 and No. DE-F603-98DP00211, and NSF Grant No. DMS-9722121. We acknowledge useful conversations with Dr. B. Afeyan, Dr. K-C. Tzeng, Dr. E. Esarey, Dr. T. Katsouleas, Dr. T. Johnston and Dr. C. D. Decker.

APPENDIX A: ALGEBRAIC MANIPULATIONS IN CALCULATING THE REDUCED LAGRANGIAN

In this appendix we give algebraic details for obtaining the reduced Lagrangian of Eq. (10). To compute the reduced Lagrangian from the exact Lagrangian, we first isolate individual terms in the exact Lagrangian,

$$\mathcal{L}_{a\perp}=\vec{\nabla}_\perp a\cdot\vec{\nabla}_\perp a^*,$$

$$\mathcal{L}_{a\tau}=-ik_0(a\partial_\tau a^*-a^*\partial_\tau a)=2k_0\,\mathrm{Im}[a\partial_\tau a^*],$$

$$\mathcal{L}_{\phi\psi}=-2(\partial_\psi\phi)^2,$$

$$\mathcal{L}_{\phi^2}=2\phi^2,$$

$$\mathcal{L}_{a^2}=2aa^*,$$

$$\mathcal{L}_c=-aa^*\phi.$$

Now, we proceed to insert the trial functions [Eqs. (6) and (7)], and carry out the transverse integrations, term by term, in the order listed. We will use the convention that an overbar denotes a term of the reduced Lagrangian, to distinguish it from the exact Lagrangian. Term by term, this results in

$$\overline{\mathcal{L}}_{a\perp}=\int d\tilde{x}_a d\tilde{y}_a\left[4\left(\frac{\tilde{x}_a^2(1+\alpha_x^2)}{w_{xa}^4}+x\Rightarrow y\right)+k_x^2+k_y^2\right]\xi\times\exp\left[-2\left(\frac{\tilde{x}_a^2}{w_{xa}^2}+\frac{\tilde{y}_a^2}{w_{ya}^2}\right)\right]$$

$$=\frac{\pi P}{2}\left(k_x^2+k_y^2+\frac{(1+\alpha_x^2)}{w_{xa}^2}+\frac{(1+\alpha_y^2)}{w_{ya}^2}\right),$$

$$\overline{\mathcal{L}}_{a\tau}=2k_0\int d\tilde{x}_a d\tilde{y}_a\left\{-\partial_\tau\chi+\left[k_x\partial_\tau x_a-\frac{\tilde{x}_a^2}{w_{xa}^2}\times\left(\partial_\tau\alpha_x-2\alpha_x\frac{\partial_\tau w_{xa}}{w_{xa}}\right)+x\Rightarrow y\right]\right\}\xi\times\exp\left[-2\left(\frac{\tilde{x}_a^2}{w_{xa}^2}+\frac{\tilde{y}_a^2}{w_{ya}^2}\right)\right]$$

$$=-\pi Pk_0\left\{\partial_\tau\chi+\left[\frac{w_{xa}^2}{4}\partial_\tau\left(\frac{\alpha_x}{w_{xa}^2}\right)-k_x\partial_\tau x_a+x\Rightarrow y\right]\right\},$$

$$\overline{\mathcal{L}}_{a^2}=\int d\tilde{x}_a d\tilde{y}_a\xi\exp\left[-2\left(\frac{\tilde{x}_a^2}{w_{xa}^2}+\frac{\tilde{y}_a^2}{w_{ya}^2}\right)\right]=\pi\frac{P}{2},$$

$$\overline{\mathcal{L}}_c=-\int dx\,dy\,\xi\Phi\exp\left[-2\left(\frac{\tilde{x}_a^2}{w_{xa}^2}+\frac{\tilde{y}_a^2}{w_{ya}^2}+\frac{\tilde{x}_\phi^2}{w_{x\phi}^2}+\frac{\tilde{y}_\phi^2}{w_{y\phi}^2}\right)\right].$$

This integral can be evaluated by completing the square in the exponent, and shifting the integration variable,

$$\overline{\mathcal{L}}_c=-\frac{\pi w_{x\phi}w_{y\phi}\Phi P\exp\left[-2\left(\frac{(x_a-x_\phi)^2}{(w_{xa}^2+w_{x\phi}^2)}+\frac{(y_a-y_\phi)^2}{(w_{ya}^2+w_{y\phi}^2)}\right)\right]}{\sqrt{(w_{xa}^2+w_{x\phi}^2)(w_{ya}^2+w_{y\phi}^2)}},$$

$$\overline{\mathcal{L}}_{\phi\psi}=-2\int d\tilde{x}_\phi d\tilde{y}_\phi\left\{(\partial_\psi\Phi)^2+\left[4\partial_\psi(\Phi^2)\frac{\tilde{x}_\phi^2}{w_{x\phi}^3}\partial_\psi w_{x\phi}+16\Phi^2\left(\frac{\tilde{x}_\phi^2}{w_{x\phi}^4}(\partial_\psi x_\phi)^2+\frac{\tilde{x}_\phi^4}{w_{x\phi}^6}(\partial_\psi w_{x\phi})^2+\frac{\tilde{x}_\phi^2\tilde{y}_\phi^2}{w_{x\phi}^3w_{y\phi}^3}(\partial_\psi w_{x\phi})(\partial_\psi w_{y\phi})\right)+x\Rightarrow y\right]\right\}\Phi\exp\left[-4\left(\frac{\tilde{x}_\phi^2}{w_{x\phi}^2}+\frac{\tilde{y}_\phi^2}{w_{y\phi}^2}\right)\right]$$

$$=-\pi\left[\frac{w_{x\phi}w_{y\phi}}{2}(\partial_\psi\Phi)^2+\frac{\partial_\psi(\Phi^2)}{4}\partial_\psi(w_{x\phi}w_{y\phi})+\Phi^2\left(\frac{3}{8}\frac{w_{y\phi}}{w_{x\phi}}(\partial_\psi w_{x\phi})^2+\frac{(\partial_\psi w_{x\phi})(\partial_\psi w_{y\phi})}{8}+\frac{w_{y\phi}}{w_{x\phi}}(\partial_\psi x_\phi)^2+x\Rightarrow y\right)\right],$$

$$\overline{\mathcal{L}}_{\phi^2}=\int d\tilde{x}_\phi d\tilde{y}_\phi\Phi^2\exp\left[-2\left(\frac{\tilde{x}_\phi^2}{w_{x\phi}^2}+\frac{\tilde{y}_\phi^2}{w_{y\phi}^2}\right)\right]=\pi[(\Phi^2w_{x\phi}w_{y\phi})/2].$$

In the above, the symbol $x\Rightarrow y$ indicates an identical expression with the variable x replaced with y, including the subscripts.

APPENDIX B: NONLINEAR EQUATIONS OF MOTION

In this appendix we give the full set of nonlinear envelope equations obtained by varying the Lagrangian density of Eq. (12). These are as follows: for, δw_{xa},

$$\frac{k_0^2}{2}\partial_\tau^2 w_{xa}-\frac{2}{w_{xa}^3}+\frac{\Phi w_{x\phi}w_{y\phi}w_{xa}[(w_{xa}^2+w_{x\phi}^2)-4(x_a-x_\phi)^2]}{(w_{xa}^2+w_{x\phi}^2)^{5/2}(w_{ya}^2+w_{y\phi}^2)^{1/2}}\exp\left[-2\left(\frac{(x_a-x_\phi)^2}{(w_{xa}^2+w_{x\phi}^2)}+\frac{(y_a-y_\phi)^2}{(w_{ya}^2+w_{y\phi}^2)}\right)\right]=0,$$

for δw_{ya},

$$\frac{k_0^2}{2}\partial_\tau^2 w_{ya}-\frac{2}{w_{ya}^3}+\frac{\Phi w_{x\phi}w_{y\phi}w_{ya}[(w_{ya}^2+w_{y\phi}^2)-4(y_a-y_\phi)^2]}{(w_{ya}^2+w_{y\phi}^2)^{5/2}(w_{xa}^2+w_{x\phi}^2)^{1/2}}\exp\left[-2\left(\frac{(x_a-x_\phi)^2}{(w_{xa}^2+w_{x\phi}^2)}+\frac{(y_a-y_\phi)^2}{(w_{ya}^2+w_{y\phi}^2)}\right)\right]=0,$$

for $\delta w_{x\phi}$,

$$(\partial_\psi\Phi)^2-\frac{1}{2}\partial_\psi^2(\Phi^2)-\frac{1}{2w_{y\phi}}\partial_\psi(\Phi^2\partial_\psi w_{y\phi})-\frac{3}{2w_{y\phi}w_{y\phi}}\partial_\psi(\Phi^2 w_{y\phi}\partial_\psi w_{x\phi})+\frac{3}{4}\Phi^2\left(\frac{(\partial_\psi w_{x\phi})^2}{w_{x\phi}^2}+\frac{(\partial_\psi w_{y\phi})^2}{w_{y\phi}^2}\right)$$
$$+2\Phi^2\left(-\frac{(\partial_\psi x_\phi)^2}{w_{x\phi}^2}+\frac{(\partial_\psi y_\phi)^2}{w_{y\phi}^2}\right)-\Phi^2+\frac{P\Phi[w_{xa}^2(w_{xa}^2+w_{x\phi}^2)+4w_{x\phi}^2(x_a-x_\phi)^2]\exp\left[-2\left(\frac{(x_a-x_\phi)^2}{(w_{xa}^2+w_{x\phi}^2)}+\frac{(y_a-y_\phi)^2}{(w_{ya}^2+w_{y\phi}^2)}\right)\right]}{(w_{ya}^2+w_{y\phi}^2)^{1/2}(w_{xa}^2+w_{x\phi}^2)^{5/2}}$$
$$=0,$$

for $\delta w_{y\phi}$,

$$(\partial_\psi\Phi)^2-\frac{1}{2}\partial_\psi^2(\Phi^2)-\frac{1}{2w_{x\phi}}\partial_\psi(\Phi^2\partial_\psi w_{x\phi})-\frac{3}{2w_{x\phi}w_{y\phi}}\partial_\psi(\Phi^2 w_{x\phi}\partial_\psi w_{y\phi})+\frac{3}{4}\Phi^2\left(\frac{(\partial_\psi w_{x\phi})^2}{w_{x\phi}^2}+\frac{(\partial_\psi w_{y\phi})^2}{w_{y\phi}^2}\right)$$
$$+2\Phi^2\left(\frac{(\partial_\psi x_\phi)^2}{w_{x\phi}^2}-\frac{(\partial_\psi y_\phi)^2}{w_{y\phi}^2}\right)-\Phi^2+\frac{P\Phi[w_{ya}^2(w_{ya}^2+w_{y\phi}^2)+4w_{y\phi}^2(y_a-y_\phi)^2]\exp\left[-2\left(\frac{(x_a-x_\phi)^2}{(w_{xa}^2+w_{x\phi}^2)}+\frac{(y_a-y_\phi)^2}{(w_{ya}^2+w_{y\phi}^2)}\right)\right]}{(w_{xa}^2+w_{x\phi}^2)^{1/2}(w_{ya}^2+w_{y\phi}^2)^{5/2}}$$
$$=0,$$

for $\delta\Phi$,

$$\frac{\partial_\psi(w_{x\phi}w_{y\phi}\partial_\psi\Phi)}{w_{x\phi}w_{y\phi}}+\frac{\Phi\partial_\psi^2(w_{x\phi}w_{y\phi})}{2w_{x\phi}w_{y\phi}}-\frac{\Phi(\partial_\psi w_{x\phi})(\partial_\psi w_{y\phi})}{2w_{x\phi}w_{y\phi}}-\frac{3\Phi}{4}\left(\frac{(\partial_\psi w_{x\phi})^2}{w_{x\phi}^2}+\frac{(\partial_\psi w_{y\phi})^2}{w_{y\phi}^2}\right)-2\Phi\left(\frac{(\partial_\psi x_\phi)^2}{w_{x\phi}^2}+\frac{(\partial_\psi y_\phi)^2}{w_{y\phi}^2}\right)+\Phi$$
$$-\frac{P\exp\left[-2\left(\frac{(x_a-x_\phi)^2}{(w_{xa}^2+w_{x\phi}^2)}+\frac{(y_a-y_\phi)^2}{(w_{ya}^2+w_{y\phi}^2)}\right)\right]}{2(w_{xa}^2+w_{x\phi}^2)^{1/2}(w_{ya}^2+w_{y\phi}^2)^{1/2}}=0,$$

for δx_a,

$$k_0^2\partial_\tau^2 x_a+\frac{2w_{x\phi}w_{y\phi}\Phi(x_a-x_\phi)\exp\left[-2\left(\frac{(x_a-x_\phi)^2}{(w_{xa}^2+w_{x\phi}^2)}+\frac{(y_a-y_\phi)^2}{(w_{ya}^2+w_{y\phi}^2)}\right)\right]}{(w_{xa}^2+w_{x\phi}^2)^{3/2}(w_{ya}^2+w_{y\phi}^2)^{1/2}}=0,$$

for δy_a,

$$k_0^2\partial_\tau^2 y_a+\frac{2w_{x\phi}w_{y\phi}\Phi(y_a-y_\phi)\exp\left[-2\left(\frac{(x_a-x_\phi)^2}{(w_{xa}^2+w_{x\phi}^2)}+\frac{(y_a-y_\phi)^2}{(w_{ya}^2+w_{y\phi}^2)}\right)\right]}{(w_{ya}^2+w_{y\phi}^2)^{3/2}(w_{xa}^2+w_{x\phi}^2)^{1/2}}=0,$$

for δx_ϕ,

$$\partial_\psi\left(\Phi^2\frac{w_{y\phi}}{w_{x\phi}}\partial_\psi x_\phi\right)-\frac{w_{x\phi}w_{y\phi}P\Phi(x_a-x_\phi)\exp\left[-2\left(\frac{(x_a-x_\phi)^2}{(w_{xa}^2+w_{x\phi}^2)}+\frac{(y_a-y_\phi)^2}{(w_{ya}^2+w_{y\phi}^2)}\right)\right]}{(w_{xa}^2+w_{x\phi}^2)^{3/2}(w_{ya}^2+w_{y\phi}^2)^{1/2}}=0,$$

for δy_ϕ,

$$\partial_\psi\left(\Phi^2\frac{w_{x\phi}}{w_{y\phi}}\partial_\psi y_\phi\right)-\frac{w_{x\phi}w_{y\phi}P\Phi(y_a-y_\phi)\exp\left[-2\left(\frac{(x_a-x_\phi)^2}{(w_{xa}^2+w_{x\phi}^2)}+\frac{(y_a-y_\phi)^2}{(w_{ya}^2+w_{y\phi}^2)}\right)\right]}{(w_{ya}^2+w_{y\phi}^2)^{3/2}(w_{xa}^2+w_{x\phi}^2)^{1/2}}=0,$$

APPENDIX C: THE QUADRATIC LAGRANGIAN

In this appendix we give the details for obtaining the quadratic Lagrangian. This is done by expanding the reduced Lagrangian in Eq. (10) about the zeroth order equilibrium solution. We make the perturbation substitutions

$$\Phi=\frac{P}{4w_0^2}+\varepsilon\Phi_1,$$

$$w_{xa}=w_0+\varepsilon w_{xa1},\quad w_{ya}=w_0+\varepsilon w_{ya1},\quad w_{x\phi}=w_0+\varepsilon w_{x\phi1},\quad w_{y\phi}=w_0+\varepsilon w_{y\phi1},$$

$$x_a=\varepsilon x_{a1},\quad y_a=\varepsilon y_{a1},\quad x_\phi=\varepsilon x_{\phi1},\quad y_\phi=\varepsilon y_{\phi1}.$$

and Taylor expand the Lagrangian to second order in ϵ. Collecting the second-order terms, we have,

$$\begin{aligned}\overline{\mathcal{L}}_2=&-\frac{16\tilde{P}}{w_0^4}(k_0^2w_0^4[(\partial_\tau x_{a1})^2+(\partial_\tau y_{a1})^2]+4\tilde{P}[(\partial_\psi x_{\phi1})^2+(\partial_\psi y_{\phi1})^2]-4P[(x_{a1}-x_{\phi1})^2+(y_{a1}-y_{\phi1})^2])-\frac{w_0^2}{2}[(\partial_\psi\Phi_1)^2-\Phi_1^2]\\&-\frac{4\tilde{P}}{w_0}[(\partial_\psi w_{x\phi1}+\partial_\psi w_{y\phi1})\partial_\psi\Phi_1-(w_{xa1}+w_{ya1}+w_{x\phi1}+w_{y\phi1})\Phi_1]-\frac{4\tilde{P}}{w_0^4}\{k_0^2w_0^4[(\partial_\tau w_{xa1})^2+(\partial_\tau w_{ya1})^2]\\&-2(6-\tilde{P})[w_{xa1}^2+w_{ya1}^2]+4\tilde{P}w_{xa1}w_{ya1}\}-\frac{8\tilde{P}^2}{w_0^4}\{3[(\partial_\psi w_{x\phi1})^2+(\partial_\psi w_{y\phi1})^2-w_{x\phi1}^2-w_{y\phi1}^2]\\&+2[(\partial_\psi w_{x\phi1})(\partial_\psi w_{y\phi1})-w_{x\phi1}w_{y\phi1}]\}-\frac{16\tilde{P}^2}{w_0^4}(w_{xa1}-w_{yal})(w_{x\phi1}-w_{y\phi1}).\end{aligned}$$

Then, making a change of variables to

$$\overline{w}_a\equiv\frac{w_{xa1}+w_{ya1}}{2},\quad \overline{w}_\phi\equiv\frac{w_{x\phi1}+w_{y\phi1}}{2},$$

$$\Delta w_a\equiv\frac{w_{xa1}-w_{ya1}}{2},\quad \Delta w_\phi\equiv\frac{w_{x\phi1}-w_{ya\phi1}}{2},$$

we can write the quadratic Lagrangian as

$$\begin{aligned}\mathcal{L}_{\Phi^2}=&-\frac{16\tilde{P}}{w_0^4}(k_0^2w_0^4[(\partial_\tau x_{a1})^2+(\partial_\tau y_{a1})^2]+4\tilde{P}[(\partial_\psi x_{\phi1})^2+(\partial_\psi y_{\phi1})^2]-4\tilde{P}[(x_{a1}-x_{\phi1})^2+(y_{a1}-y_{\phi1})^2])\\&-\frac{w_0^2}{2}[(\partial_\psi\Phi_1)^2-\Phi_1^2]-\frac{8\tilde{P}}{w_0}[(\partial_\psi\overline{w}_\phi)\partial_\psi\Phi_1-(\overline{w}_a+\overline{w}_\phi)\Phi_1]-\frac{32\tilde{P}}{w_0^4}\{x_R^2(\partial_\tau\overline{w}_a)^2-(3-\tilde{P})\overline{w}_a^2+2\tilde{P}[(\partial_\psi\overline{w}_\phi)^2-\overline{w}_\phi^2]\}\\&-\frac{32\tilde{P}}{w_0^4}\{x_R^2(\partial_\tau\Delta w_a)^2-3\Delta w_a^2+\tilde{P}[(\partial_\psi\Delta w_\phi)^2-\Delta w_\phi^2+2\Delta w_\phi\Delta w_a]\},\end{aligned}$$

where $x_R=k_0w_0^2/2$, $\tilde{P}\equiv P/P_{\rm crit}$. This can then broken up into individual pieces, as is done in Eq. (17)–(20).

[1] T. Tajima and J. M. Dawson, Phys. Rev. Lett. **43**, 267 (1979); E. Esarey *et al.*, IEEE Trans. Plasma Sci. **24**, 252 (1996), and references therein.
[2] Special issue of IEEE Trans. Plasma Sci. PS-21(1) (1993), edited by W. B. Mori.
[3] M. Tabek *et al.*, Phys. Plasmas **1**, 1626 (1994).
[4] W. B. Mori, IEEE J. Quantum Electron. **33**, 1942 (1997) and references therein.
[5] W. B. Mori *et al.*, Phys. Rev. Lett. **72**, 1482 (1994); C. D. Decker *et al.*, Phys. Plasmas **3**, 414 (1996); C. D. Decker *et al.*, Phys. Rev. E **50**, R3338 (1994).
[6] A. S. Sakharov and V. I. Kirsanov, Phys. Rev. E **49**, 3274 (1994).
[7] E. Esarey *et al.*, Phys. Rev. Lett. **72**, 2887 (1994).
[8] P. Sprangle *et al.*, Phys. Rev. Lett. **69**, 2200 (1992).
[9] T. M. Antonsen, Jr. and P. Mora, Phys. Rev. Lett. **69**, 2204 (1992); P. Mora and T. Anotonsen, Jr., Phys. Fluids B **5**, 1440 (1993).
[10] N. E. Andreev *et al.*, Pis'ma Zh. Eksp. Teor. Fiz. **55**, 551 (1992) [JETP LETT. **55**, 571 (1992)].
[11] P. Sprangle *et al.*, Phys. Rev. Lett. **73**, 3544 (1994).
[12] G. Shvets and J. S. Wurtele, Phys. Rev. Lett. **73**, 3540 (1994).
[13] D. Anderson and M. Bonnedal, Phys. Fluids **22**, 105 (1979).
[14] J. F. Lam *et al.*, Opt. Commun. **15**, 419 (1975); J. F. Lam *et al.*, Phys. Fluids **20**, 1176 (1977).
[15] P. Sprangle *et al.*, Phys. Rev. A **36**, 2773 (1987); E. Esarey *et al.*, IEEE J. Quantum Electron. **33**, 1879 (1997).
[16] X. L. Chen and R. N. Sudan, Phys. Fluids B **5**, 1336 (1993); X. L. Chen and R. N. Sudan, Phys. Rev. Lett. **70**, 2082 (1993).
[17] K.-C. Tzeng and W. B. Mori (unpublished).
[18] B. J. Duda, R. G. Hemker, K. C. Tzeng, and W. B. Mori, Phys. Rev. Lett. **83**, 1978 (1999).
[19] C. J. McKinstrie and R. Bingham, Phys. Fluids B **4**, 2626 (1992); C. E. Max *et al.*, Phys. Rev. Lett. **33**, 209 (1974).
[20] J. Killingbeck and G. H. A. Cole, *Mathematical Techniques and Physical Applications* (Academic, New York, 1971).
[21] J. Schwinger *et al.*, *Classical Electrodynamics* (Perseus Books, Reading, Mass, 1998).
[22] C. A. Coverdale *et al.*, Phys. Rev. Lett. **74**, 4659 (1995).
[23] A. Modena *et al.*, Nature (London) **337**, 606 (1995); D. Gordon *et al.*, Phys. Rev. Lett. **80**, 2133 (1997).
[24] K. Nakajima *et al.*, Phys. Rev. Lett. **74**, 4428 (1995).
[25] D. Umstadter *et al.*, Science **273**, 472 (1996).
[26] C. I. Moore *et al.*, Phys. Rev. Lett. **79**, 3909 (1997).
[27] D. Whittum *et al.*, Phys. Rev. Lett. **67**, 991 (1991); M. Lampe *et al.*, Phys. Fluids B **5**, 1888 (1993).
[28] R. L. Seliger and G. B. Whitham, Proc. R. Soc. London, Ser. A **305**, 1 (1968).
[29] R. W. Atherton and G. M. Homsy, Stud. Appl. Math. **54**, 31 (1975).
[30] M. M. Vainberg, *Variational Methods for the Study of Nonlinear Operators* (Holden-Day, San Francisco, 1964).
[31] A. J. Brizard, Phys. Plasmas **5**, 1110 (1998).
[32] W. B. Mori *et al.*, Bull. Am. Phys. Soc. **44**, 179 (1999).